

The HvNramp5 Transporter Mediates Uptake of Cadmium and Manganese, But Not Iron¹[OPEN]

Dezhi Wu, Naoki Yamaji, Miki Yamane, Miho Kashino-Fujii, Kazuhiro Sato, and Jian Feng Ma*

Institute of Plant Science and Resources, Okayama University, Kurashiki 710-0046, Japan (D.W., N.Y., M.Y., M.K., K.S., J.F.M.); and Department of Agronomy, Zhejiang University, Hangzhou 310058, China (D.W.)

ORCID IDs: 0000-0001-8818-5203 (K.S.); 0000-0003-3411-827X (J.F.M.).

The Natural Resistance Associated Macrophage Protein (Nramp) represents a transporter family for metal ions in all organisms. Here, we functionally characterized a member of Nramp family in barley (*Hordeum vulgare*), HvNramp5. This member showed different expression patterns, transport substrate specificity, and cellular localization from its close homolog in rice (*Oryza sativa*), OsNramp5, although HvNramp5 was also localized to the plasma membrane. HvNramp5 was mainly expressed in the roots and its expression was not affected by Cd and deficiency of Zn, Cu, and Mn, but slightly up-regulated by Fe deficiency. Spatial expression analysis showed that the expression of HvNramp5 was higher in the root tips than that in the basal root regions. Furthermore, analysis with laser microdissection revealed higher expression of HvNramp5 in the outer root cell layers. HvNramp5 showed transport activity for both Mn²⁺ and Cd²⁺, but not for Fe²⁺ when expressed in yeast. Immunostaining with a HvNramp5 antibody showed that this protein was localized in the root epidermal cells without polarity. Knockdown of HvNramp5 in barley resulted in a significant reduction in the seedling growth at low Mn supply, but this reduction was rescued at high Mn supply. The concentration of Mn and Cd, but not other metals including Cu, Zn, and Fe, was decreased in both the roots and shoots of knockdown lines compared with the wild-type barley. These results indicate that HvNramp5 is a transporter required for uptake of Mn and Cd, but not for Fe, and that barley has a distinct uptake system from rice.

Transport of mineral elements from soil to different organs and tissues of plants requires different types of transporters (Hall and Williams, 2003; Nevo and Nelson, 2006; Yokosho et al., 2009; Olsen and Palmgren, 2014; Sasaki et al., 2016), which include the zinc-regulated transporters, iron-regulated transporter-like protein family; the natural resistance-associated macrophage protein (Nramp) family of transporters; the multidrug and toxic compound extrusion protein transporters; the heavy metal ATPase transporters; the oligopeptide transporters family; the ATP-binding

cassette family of transporters; and the cation-diffusion facilitator family of transporters. Among them, Nramp represents a transporter family for metal ion in all organisms including bacteria, animals, and plants (Curie et al., 2000; Nevo and Nelson, 2006). Some members of this family in plants have been functionally characterized, especially in model plants such as Arabidopsis (*Arabidopsis thaliana*) and rice (*Oryza sativa*). In Arabidopsis, there are six members of Nramp transporter proteins. AtNramp1 is localized to the plasma membrane of root cells and functions as a high-affinity transporter for Mn uptake (Cailliatte et al., 2010). Both AtNramp3 and AtNramp4 are localized to the tonoplast and play redundant roles in Fe, exporting from the vacuole during seed germination and in Mn homeostasis at the adult stage (Thomine et al., 2000; Lanquar et al., 2005, 2010). AtNramp6 is targeted to a vesicular-shaped endomembrane compartment and is implicated in the distribution or availability of Cd within cells (Cailliatte et al., 2009). However, the function of AtNramp2 and AtNramp5 has not been characterized.

On the other hand, there are seven members of Nramp transporter family in the rice genome, of which four have been functionally characterized. They all are localized to the plasma membrane but show different roles. OsNramp1 shows transport activity for Fe and Cd in yeast and is proposed to be involved in Cd accumulation (Takahashi et al., 2011). OsNramp3 is localized at the vascular tissues of nodes and plays an important role in distribution of Mn, but not Fe and Cd (Yamaji et al., 2013). On the other hand, OsNramp1

¹ This work was supported by a grant from the Ministry of Agriculture, Forestry, and Fisheries of Japan (Genomics-based Technology for Agricultural Improvement grant no. TRS-1006 and the Scientific Technique Research Promotion Program for Agriculture, Forestry, Fisheries and Food Industry grant no. 25013A to J.F.M.) and by a Grant-in-Aid for Specially Promoted Research (Japan Society for the Promotion of Science KAKENHI grant no. 16H06296 to J.F.M.).

* Address correspondence to maj@rib.okayama-u.ac.jp.

The author responsible for distribution of materials integral to the findings presented in this article in accordance with the policy described in the Instructions for Authors (www.plantphysiol.org) is: Jian Feng Ma (maj@rib.okayama-u.ac.jp).

D.W. and J.F.M. designed the experiments and wrote the article; N.Y. assisted with immunostaining experiments; M.Y. and K.S. assisted with barley transformation; M.K.-F. assisted with laser microdissection assay; J.F.M. planned the project, and designed and supervised the experiments; all authors discussed the results and commented on the article.

[OPEN] Articles can be viewed without a subscription.

www.plantphysiol.org/cgi/doi/10.1104/pp.16.01189

(OsNramp4) transports trivalent Al ion (Xia et al., 2010) and is required for high Al tolerance in rice roots. Finally, OsNramp5 functions as a major transporter responsible for root Mn and Cd uptake (Ishimaru et al., 2012; Ishikawa et al., 2012; Sasaki et al., 2012). However, the function of OsNramp2, OsNramp6, and OsNramp7 is unknown.

In addition to Nramp members characterized in rice and Arabidopsis, some members in other plant species have also been characterized. For example, a soybean (*Glycine max*) Nramp transporter, GmDMT1 is implicated in the ferrous iron transport (Kaiser et al., 2003). Nramp1 isolated from *Nocca caerulea*, a Zn/Cd hyperaccumulator, is involved in the influx of Cd across the endodermal plasma membrane and plays a key role in Cd flux into the stele and root-to-shoot Cd transport (Milner et al., 2014). In *Malus baccata*, Nramp1 is capable of mediating the distribution of ions as well as transport of Fe, Mn, and Cd (Xiao et al., 2008). Besides, Nramp1 and Nramp3 in tomato (*Solanum lycopersicum*) have also been suggested to be involved in Mn transport (Bereczky et al., 2003). When *NcNramp3* and *NcNramp4* from *Nocca caerulea* were expressed in yeast, *NcNramp3* transported Fe, Mn, and Cd, while *NcNramp4* also transported Zn in addition to Fe, Mn, and Cd (Oomen et al., 2009). However, Nramp4 isolated from *Thlaspi japonicum*, a Ni hyperaccumulator, showed transport activity for Ni but not for Zn, Cd, or Mn in yeast (Mizuno et al., 2005). These findings indicate that Nramp members have a diverse role in metal transport in plants.

Barley (*Hordeum vulgare*) is the fourth most important cereal crop in the world; however, less progress has been made in understating of molecular mechanisms on mineral element transport in barley due to its large genome size. For example, no Nramp members in barley have been functionally characterized so far. In this study, we first isolated barley Nramp member, HvNramp5, which is a close homolog of rice OsNramp5. Detailed functional analysis revealed that HvNramp5 is involved in the uptake of both Mn and Cd, but not of Fe in barley roots. Furthermore, we found that different from OsNramp5, HvNramp5 showed a distinct pattern in the gene expression, cellular localization, and transport substrate.

RESULTS

Isolation and Phylogenetic Analysis of HvNramp5

The full-length cDNA of *HvNramp5* in barley cultivar Golden Promise was amplified by PCR using primers designed based on database information (AK364374; <http://www.ncbi.nlm.nih.gov/nucore/AK364374>). Blast search revealed that one copy of *HvNramp5* is present in the barley genome (http://plants.ensembl.org/Hordeum_vulgare/Info/Index). Sequence analysis showed that the full-length cDNA of *HvNramp5* contains 1638 bp, which encodes a peptide with

545 amino acids (Supplemental Fig. S1A). Comparison of the cDNA sequence with a genomic DNA sequence obtained from the released barley genome (Mayer et al., 2012) revealed that *HvNramp5* comprises 11 introns and 12 exons (Supplemental Fig. S1B). *HvNramp5* showed 39% to 84% identity with rice Nramp members (Supplemental Fig. S1C) and the closest one is OsNramp5 (84%). *HvNramp5* is predicted as a membrane protein with 11 transmembrane domains (Supplemental Fig. S1D).

Expression Patterns of HvNramp5

Expression analysis with quantitative RT-PCR showed that *HvNramp5* was mainly expressed in the roots (Fig. 1A). The expression in the roots was not affected by deficiency of Mn, Cu, and Zn, but slightly up-regulated by Fe deficiency. The expression was also

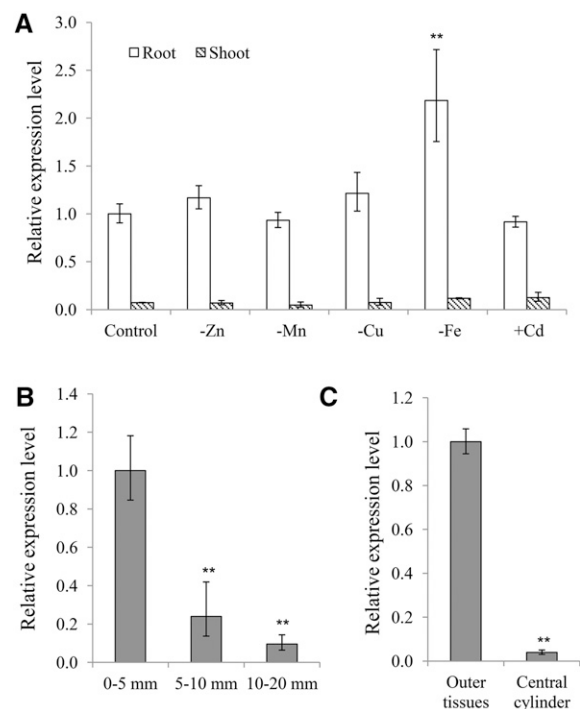


Figure 1. Expression pattern of *HvNramp5*. A, Expression of *HvNramp5* in response to metal deficiency or Cd. The seedlings of barley cultivar Golden Promise were cultivated in a one-fifth Hoagland's solution with (control) or without Zn, Mn, Cu, or Fe or with 0.5 μM Cd. After 7-d treatments, the roots and shoots were sampled for RNA extraction. B, Spatial expression of *HvNramp5* along the roots of Golden Promise. RNA was extracted from the root tip (0–5 mm), root elongation zone (5–10 mm), or root hair zone (10–20 mm) from 7-d-old barley roots. C, Tissue-specificity of expression of *HvNramp5*. Different tissues were sampled from the roots (2 mm from root tip) of barley (cv Morex) using a Veritas Laser Microdissection System as described by Fujii et al. (2012). The expression level was determined by quantitative real-time RT-PCR and expression relative to the control root (A), root tip (B), and outer tissues (C) is shown. Data are means \pm SD of three biological replicates and asterisks indicate significant difference at $**P < 0.01$ by Student's *t* test.

not affected by Cd exposure (Fig. 1A). Spatial expression analysis showed that the expression of *HvNramp5* was markedly higher in the root tips (0 mm to 5 mm) than in the root elongation zone (5 mm to 10 mm) and root hair zone (10 mm to 20 mm; Fig. 1B). Furthermore, we investigated tissue-specificity of expression of *HvNramp5* using the sample prepared before with help of laser microdissection in the root tips (2 mm; Fujii et al., 2012). The result showed that *HvNramp5* was highly expressed in the outer root cell layer compared with the central cylinder tissues (Fig. 1C).

HvNramp5 Transports Mn and Cd, But Not Fe, in Yeast

To examine transport activity of *HvNramp5* for metals, we expressed an *HvNramp5*, *HvIRT1*, or *pYES2*

empty vector in different yeast strains, respectively. *HvIRT1* as a positive control is known to transport Mn^{2+} , Fe^{2+} , and Cd^{2+} in yeast (Padas et al., 2008). In a yeast mutant defective in Mn uptake, $\Delta smf1$, expression of *HvNramp5* and *HvIRT1* rescued the yeast growth under Mn-limited condition induced by Mn-chelator ethylene glycol tetraacetic acid (EGTA), but expression of the vector alone did not rescue the growth (Fig. 2A). By contrast, expression of *HvNramp5* and the vector control was not able to complement the growth in a yeast mutant DDY4 ($\Delta fet3fet4$) defective in Fe uptake, whereas expression of *HvIRT1* rescued the yeast growth, under Fe(II)-limited condition generated by Fe(II)-chelator 4,7-biphenyl-1,10-phenanthroline-disulphonic acid (BPDS; Fig. 2B). On the other hand, the growth of yeast strain BY4741 (a wild-type strain) expressing *HvNramp5* and

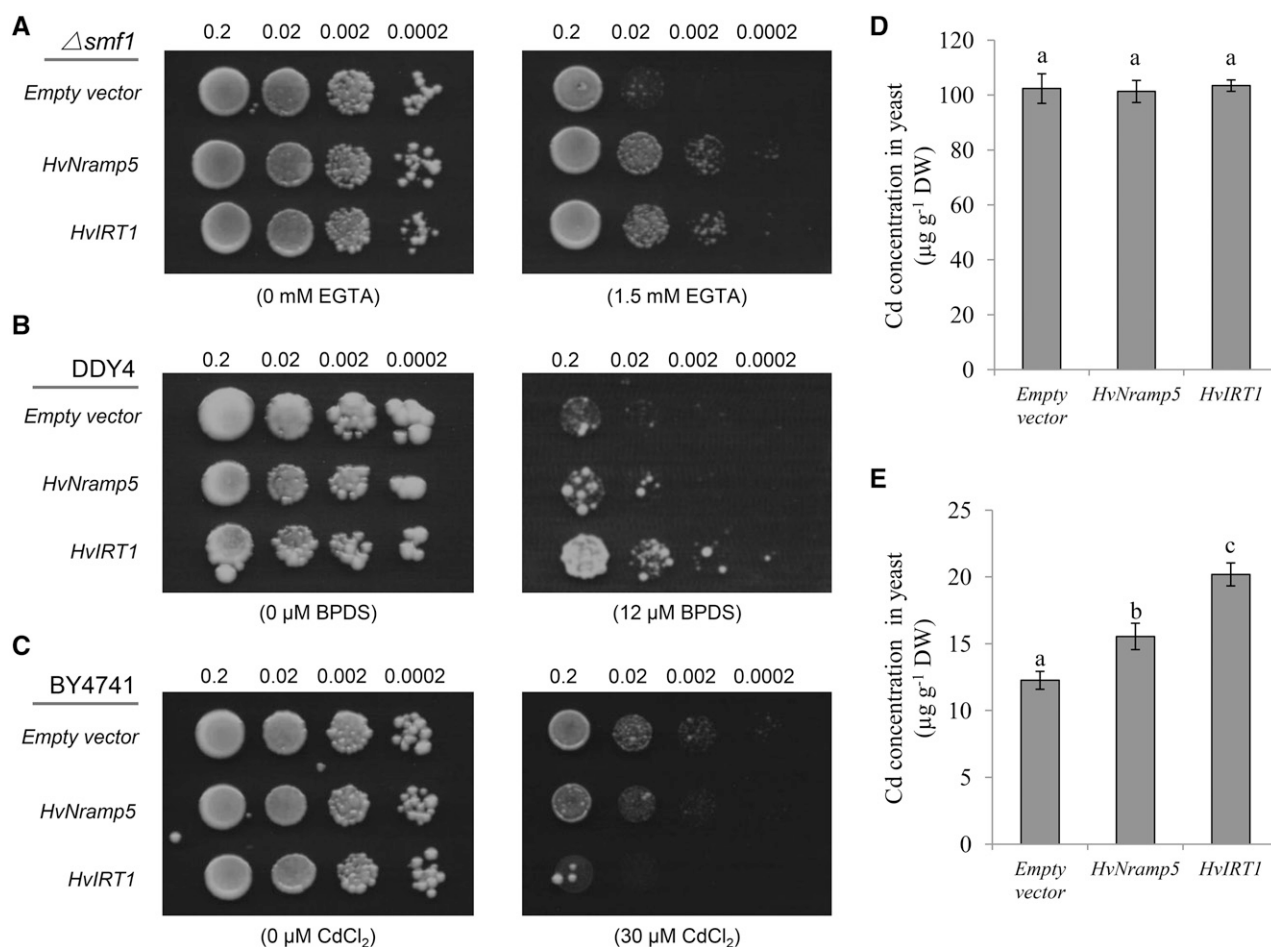


Figure 2. Metal transport activity assay of *HvNramp5* in yeast. A, Functional complementation for Mn uptake in the strain $\Delta smf1$. B, Functional complementation for Fe uptake in the strain DDY4 ($\Delta fet3fet4$). C, Sensitivity test to Cd toxicity in the strain BY4741. Different yeast strains carrying *HvNramp5*, *HvIRT1*, or empty vector (*pYES2*) were cultured on the plate with or without Mn-chelator EGTA (A), Fe-chelator BPDS (B), or Cd (C). Eight microliters of cell suspension with an OD_{600nm} of 0.2 and three serial 1:10 dilutions were spotted and incubated at 30°C for 3 to 5 d. D to E, Cd uptake in liquid medium. Yeast BY4741 carrying *HvNramp5*, *HvIRT1*, or empty vector (*pYES2*) was cultured in a liquid medium containing 2% Glc (D) or Gal (E) in the presence of 5 μM $CdCl_2$ for 4 h. The Cd concentration in the yeast was determined with ICP-MS after digestion. Data are means \pm SD of three biological replicates and a different small letter indicates significant difference at $P < 0.05$ by Tukey's test.

HvIRT1 was seriously inhibited by the presence of Cd compared with that of the vector control (Fig. 2C).

The Cd accumulation in the yeast cells was also compared under the control of Gal-inducible promoter using liquid culture. The Cd accumulation in the yeast did not differ among yeast expressing *HvNramp5*, *HvIRT1*, and an empty vector in the presence of Glc (Fig. 2D), when the gene was not induced. By contrast, in the presence of Gal, yeast expressing *HvNramp5* and *IRT1* significantly accumulated higher Cd compared with the vector control (Fig. 2E). Furthermore, yeast expressing *HvIRT1* accumulated higher Cd than that expressing *HvNramp5*. This result is consistent with the growth test (Fig. 2C); the growth was inhibited more in the yeast expressing *HvIRT1* than that expressing *HvNramp5*. All these results indicate that *HvNramp5* is able to transport Mn^{2+} and Cd^{2+} , but not Fe^{2+} in yeast. Yeast cultured with Glc showed higher Cd accumulation than that cultivated with Gal (Fig. 2, D and E). This phenomenon was also reported previously by Engl and Kunz (1995), but the exact reason is unknown. Different carbon sources may affect Cd accumulation through

affecting yeast growth, cell wall components, and energy metabolism.

Cellular and Subcellular Localization of *HvNramp5*

To determine the tissue and cellular localization of *HvNramp5* in barley root, we conducted an immunostaining using an antibody against *HvNramp5*. Consistent with the expression patterns of *HvNramp5* (Fig. 1B), the signal (red) was much stronger in the root tips than in the basal root region (Fig. 3, A and C). Furthermore, *HvNramp5* was mainly localized at the epidermal cells of the root tips (Fig. 3A) although a weak signal was also detected in the central cylinder.

Immunostaining analysis also showed that *HvNramp5* is likely localized to the plasma membrane (Fig. 3B). To confirm this, we transiently expressed *HvNramp5* fused with GFP or GFP alone, together with RFP (red fluorescence protein) as a cytosolic and nuclear marker in onion epidermal cells. The green fluorescence signal from GFP was observed at the plasma membrane in

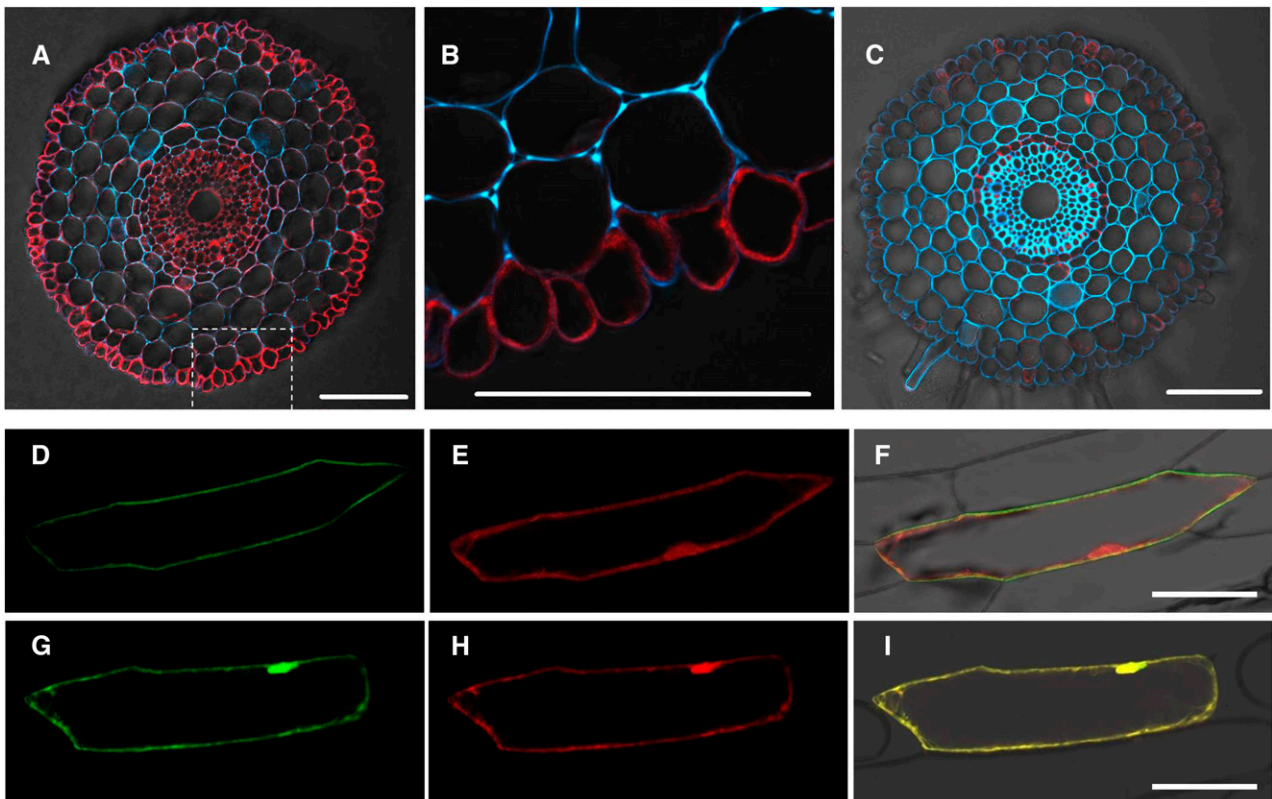


Figure 3. Cellular and subcellular localization of *HvNramp5*. A to C, Cellular localization of *HvNramp5* in barley roots. Immunostaining with *HvNramp5* antibody was performed in root tips (A and B, 2 mm from root tips) and basal roots (C, 15 mm from root tips) of barley (cv Golden Promise). B, High-magnification image of dotted part in A. Red color shows signal from the antibody, while blue color shows autofluorescence of cell wall. Bars = 100 μ m. D to I, Subcellular localization of *HvNramp5*. Confocal images of onion epidermis cells coexpressing *HvNramp5*-GFP and RFP observed with the GFP (D), RFP (E), and their merged (F) channels, and coexpressing GFP alone and RFP observed with the GFP (G), RFP (H), and their merged (I) channels. Bars = 100 μ m.

cells expressing *HvNramp5-GFP* fusion, while the red signal from RFP was localized in the cytosol and the nucleus (Fig. 3, D to F). By contrast, the signal of both green and red fluorescence was localized in the cytosol and the nucleus in the cells expressing GFP alone (Fig. 3, G–I). These results indicate that *HvNramp5* is a plasma membrane-localized transporter.

Phenotypic Analysis of *HvNramp5* Knockdown Lines

To understand the role of *HvNramp5* in barley, we generated two independent knockdown lines of *HvNramp5* using RNA interference (RNAi) methods. The expression level of *HvNramp5* in two RNAi lines was 26.1% and 37.5% of the wild-type barley (Supplemental Fig. S2A). By contrast, the expression of *HvIRT1* was not affected in the knockdown lines (Supplemental Fig. S2B).

The growth was compared between the RNAi lines and the wild types (a nontransgenic line and a line showing wild-type genotype isolated from T2 population)

when grown in a nutrient solution containing different Mn, Cd, and Fe concentrations. The root length and dry weight of the roots and shoots of the RNAi lines were significantly inhibited at low Mn ($0.05 \mu\text{M}$) compared with that of the wild types (Fig. 4, A and D). However, at higher Mn concentrations ($0.5 \mu\text{M}$ and $5 \mu\text{M}$), the difference in the growth was not observed (Fig. 4, B, C, E, and F). By contrast, the growth difference of the RNAi lines and wild types was not found between low and high concentrations of Cd and Fe (Supplemental Figs. S4 and S5).

Metal Analysis of *HvNramp5* Knockdown Lines

Analysis of metal concentration in the roots and shoots showed that the Mn concentration increased with increasing Mn concentrations in the nutrient solution in both RNAi lines and wild types (Fig. 5, A and B). However, the RNAi lines always showed a lower Mn concentration in both the roots and shoots than did

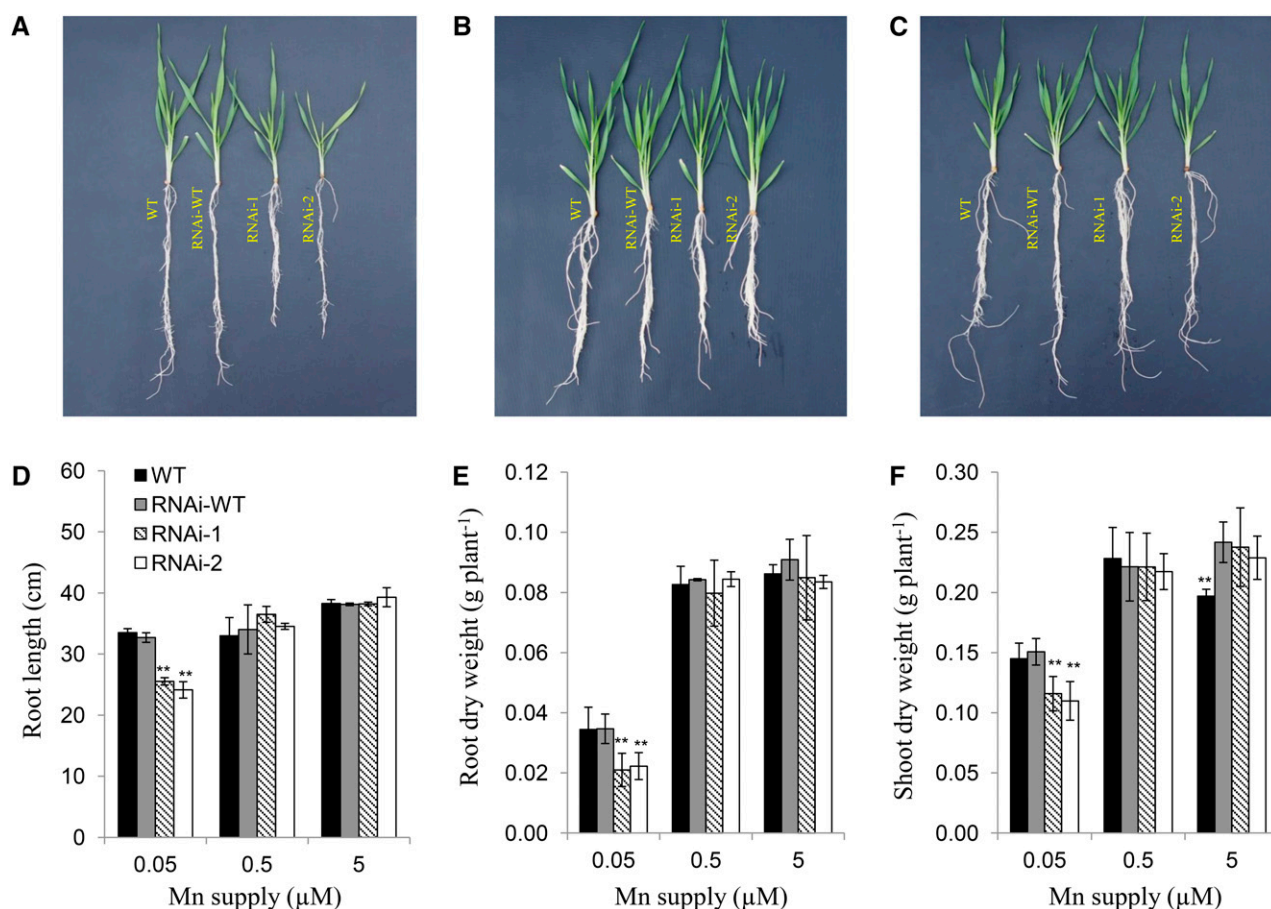


Figure 4. Effect of knockdown of *HvNramp5* on plant growth at different Mn concentrations. A to C, Growth of wild-type barley (cv Golden Promise), the homozygous wild type (RNAi-wild type), and two homozygous transgenic RNAi lines (RNAi-1, RNAi-2) derived from two independent events. All lines were cultivated in a nutrient solution containing 0.05 (A), 0.5 (B), and $5 \mu\text{M}$ (C) Mn in the presence of $0.1 \mu\text{M}$ Cd for 14 d. D to F, Root length (D) and dry weight of roots (E) and shoots (F) in these lines were recorded at harvest. Data are means \pm SD of three biological replicates and ** indicates significant difference at $P < 0.01$ by Tukey's test.

the wild types. By contrast, there was no difference in the concentration of Fe, Cu, and Zn in both the roots and shoots between the RNAi lines and wild types (Fig. 5, C and D, and Supplemental Fig. S3). Interestingly, the Cd concentration in both the roots and shoots was decreased with increasing external Mn concentrations in the wild types, but not in the RNAi lines (Fig. 5, E and F). However, the RNAi lines showed lower Cd concentration of both the roots and shoots than did the wild types at either of the Mn concentrations (Fig. 5, E and F).

When the seedlings of the RNAi lines and the wild types were exposed to different Cd concentrations (0.1, 0.5, and 1 μM), the concentration of Mn in the roots and shoots was decreased with increasing Cd concentrations in the external solution in both the RNAi lines and the wild types (Fig. 6, A and B). However, compared with the wild type, the Mn concentration in the RNAi lines was lower at either of the Cd concentrations (Fig. 6, A and B). There was almost no difference in the

concentration of Cu and Zn in both the roots and shoots between the knockdown lines and wild types (Supplemental Fig. S4), but Fe concentration in the roots and shoots was slightly higher in RNAi lines than in wild types at 1 μM Cd (Fig. 6, C and D). The reason for this increased Fe accumulation is unknown. By contrast, the concentration of Cd in the roots and the shoots was lower in knockdown lines than in wild types, although the Cd concentration of the roots and shoots increased with increasing external Cd concentrations in both the RNAi lines and wild types (Fig. 6, E and F). When the seedlings of the RNAi lines and the wild types were exposed to different Fe concentrations (0.1, 2, and 10 μM), the Fe concentration in the roots and shoots did not differ between different lines although the Fe concentration in all lines increased with increasing Fe concentrations in the external solution (Supplemental Fig. S5). These results indicate that knockdown of *HvNramp5* expression caused decreased accumulation

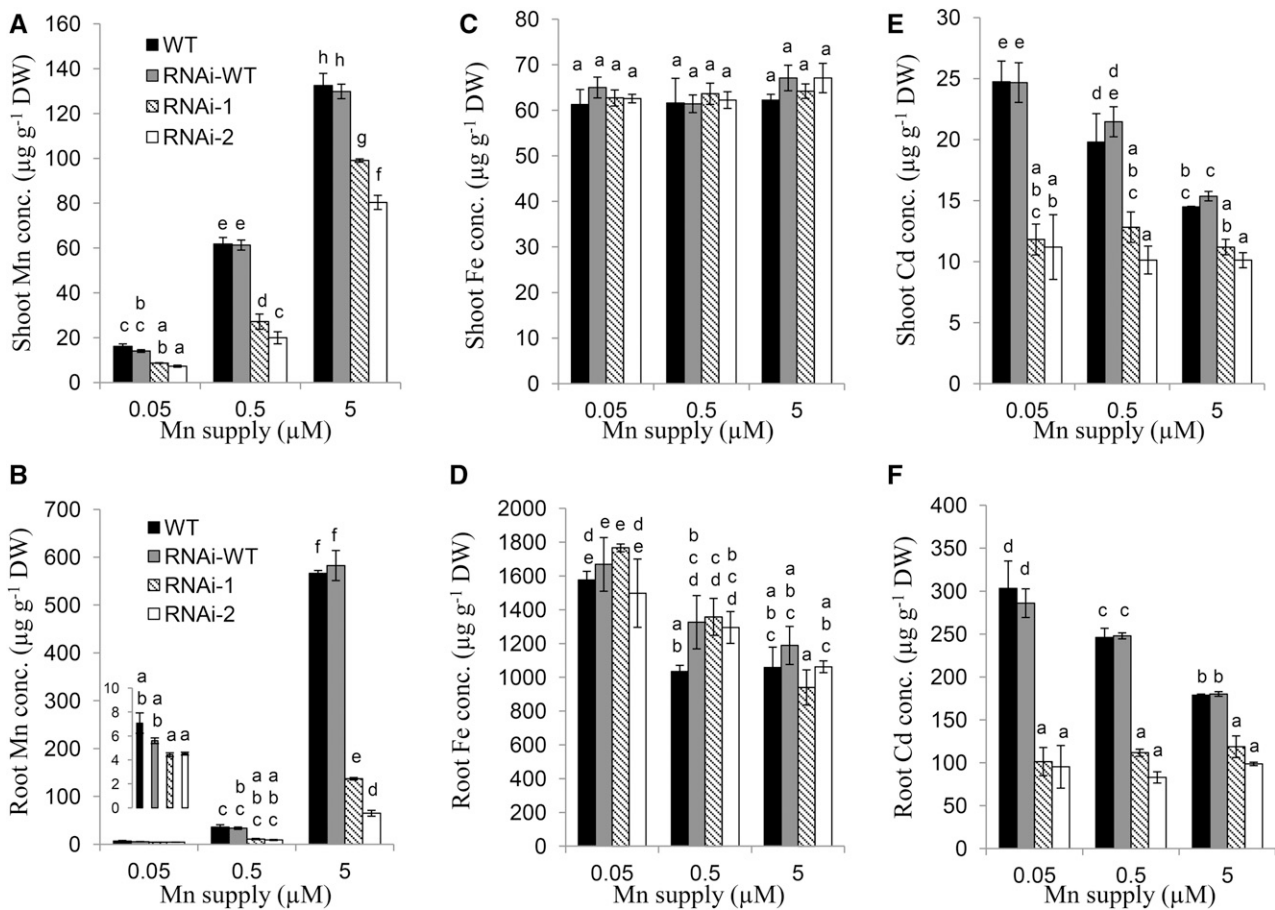


Figure 5. Metal concentration in *HvNramp5* RNAi lines at different Mn concentrations. Wild-type barley (cv Golden Promise), the homozygous wild type (RNAi-wild type), and two homozygous transgenic RNAi lines (RNAi-1, RNAi-2) derived from two independent events were cultivated in a nutrient solution containing 0.05, 0.5, and 5 μM Mn in the presence of 0.1 μM Cd for 14 d. The concentration of Mn (A and B), Fe (C and D), and Cd (E and F) in the shoots (A, C, and E) and roots (B, D, and F) was determined by ICP-MS. Data are means \pm SD of three biological replicates and a different small letter indicates significant difference at $P < 0.05$ by Tukey's test.

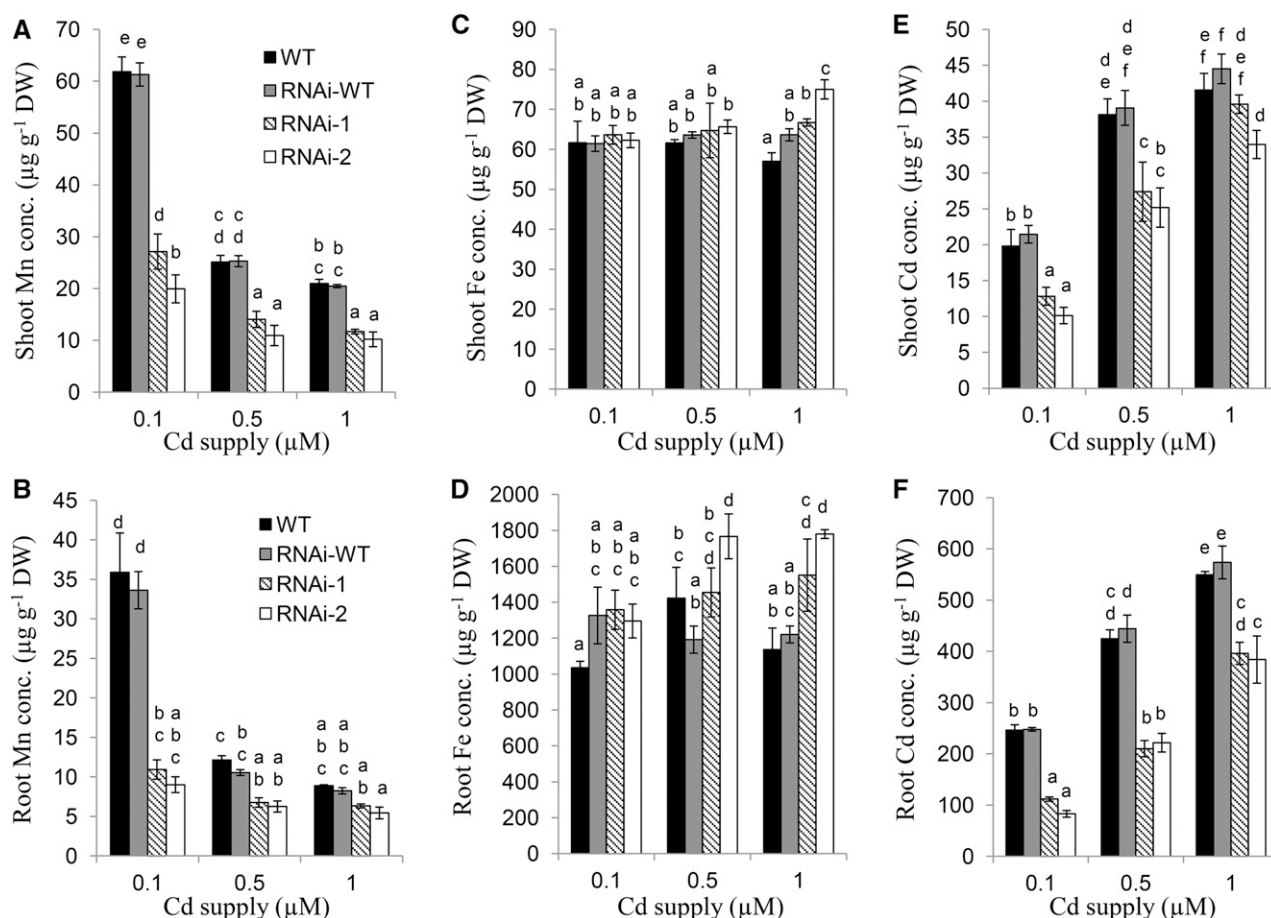


Figure 6. Metal concentration in *HvNramp5* RNAi lines at different Cd concentrations. Wild-type barley (cv Golden Promise), the homozygous wild type (RNAi-wild type), and two homozygous transgenic RNAi lines (RNAi-1, RNAi-2) derived from two independent events were cultivated in a nutrient solution containing 0.1, 0.5, or 1 μM Cd for 14 d. The concentration of Mn (A and B), Fe (C and D), and Cd (E and F) in the shoots (A, C, and E) and roots (B, D, and F) was determined by ICP-MS. Data are means \pm SD of three biological replicates and a different small letter indicates significant difference at $P < 0.05$ by Tukey's test.

of Mn and Cd, but not Fe—and that Mn and Cd competed with each other in the uptake.

Comparison of Mn Accumulation and *Nramp5* Expression between Rice and Barley

To compare differences in Mn accumulation and expression of *HvNramp5* and *OsNramp5* between barley (cv Golden Promise) and rice (cv Nipponbare), we grew both plants in a different Mn supply for one week. Barley roots accumulated higher Mn than rice roots, but rice shoots accumulated much higher Mn than did barley shoots, irrespectively of external Mn concentrations (Fig. 7, A and B). The total uptake of Mn of rice was 3 times to 6 times higher than that of barley under different Mn concentrations (Fig. 7C). The expression of *HvNramp5* and *OsNramp5* in the roots was compared between rice and barley by absolute quantitative RT-PCR. The expression of *Nramp5* was 4 times to 7 times higher in rice than in barley at all Mn supply conditions tested (Fig. 8).

DISCUSSION

HvNramp5 Is a Transporter for Uptake of Mn and Cd, But Not Fe, in Barley

In this study, we isolated and functionally characterized the first Nramp member, *HvNramp5* in barley. *HvNramp5* encodes a plasma membrane-localized protein and transports Mn^{2+} and Cd^{2+} , but not Fe^{2+} in yeast (Figs. 2 and 3). *HvNramp5* is mainly localized at the epidermal cells of the root tips (Fig. 3A). Knockdown of *HvNramp5* resulted in decreased accumulation of Mn and Cd, but not Fe, Cu, and Zn in both roots and shoots (Fig. 5 and Supplemental Fig. S3). Furthermore, the growth of knockdown lines was inhibited at low Mn concentration (Fig. 4A). These results indicate that *HvNramp5* is involved in the uptake of Mn and Cd in barley.

Mn uptake was previously reported to be mediated by HvIRT1 (Pedas et al., 2008). HvIRT1 is also a plasma membrane-localized protein and is able to transport Mn, Fe, Zn, and Cd in yeast. The expression of *HvIRT1*

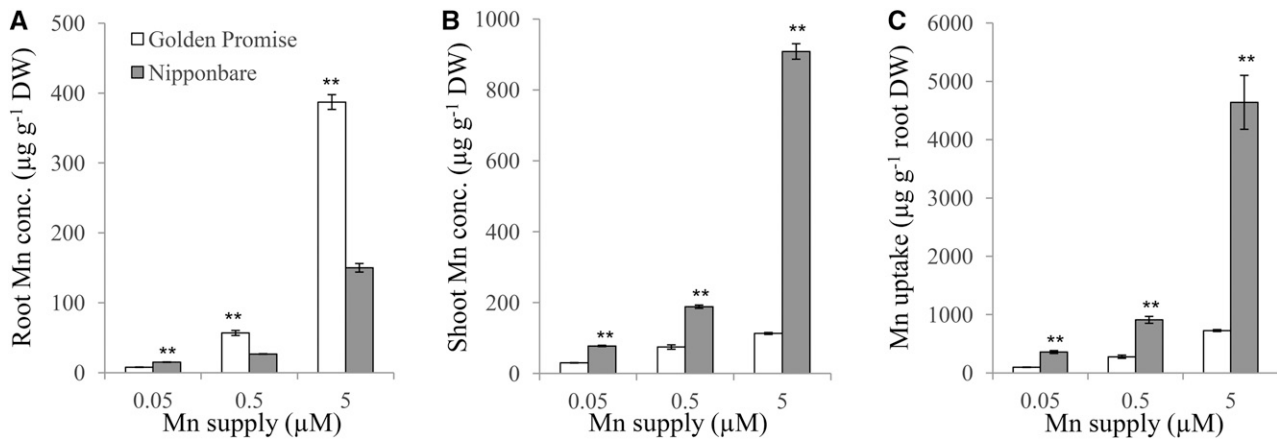


Figure 7. Accumulation of Mn in barley and rice. Concentration of Mn in the roots (A) and shoots (B) and total uptake of Mn (C) in barley (cv Golden Promise) and rice (cv Nipponbare). Rice and barley were grown in nutrient solutions containing 0.05, 0.5, or 5 μM Mn for 7 d. The concentration of Mn in the roots and shoots was determined by ICP-MS. Total uptake of Mn was calculated as total Mn content in the whole plant divided by the root dry weight. Data are means \pm SD of three biological replicates and ** indicates significant difference at $P < 0.01$ by Student's t test.

was induced by Mn and Fe-deficiency (Pedas et al., 2008). Furthermore, different *HvIRT1* expression level was associated with genotypic difference in Mn-uptake efficiency of barley (Pedas et al., 2008). However, the exact role of *HvIRT1* in Mn uptake in planta has not been examined. In this study, we found that knock-down of *HvNramp5* did not affect the expression of *HvIRT1* (Supplemental Fig. S2), but significantly reduced Mn uptake at all Mn supply conditions tested (Fig. 5, A and B). The growth of RNAi lines was inhibited at limited Mn supply (Fig. 4A). This strongly supports that *HvNramp5* is involved in Mn uptake in barley. One possibility is that *HvNramp5* and *HvIRT1* may play different roles in Mn uptake in barley. *HvIRT1* was up-regulated by Mn-deficiency (Pedas et al., 2008), while *HvNramp5* was constitutively expressed in the roots (Fig. 1A). Therefore, *HvNramp5* may constitutively contribute to Mn uptake, while *HvIRT1* may play an additional role in Mn uptake under a Mn-deficiency condition, although further works are required to make this conclusion. *HvNramp5* was also detected in the central cylinder in addition to the epidermal cells (Fig. 3A). This implicates that *HvNramp5* may also be involved in the root-to-shoot translocation of Mn, although further evidence is required.

There is worldwide concern regarding Cd accumulation in cereal grains because the intake of Cd from grains through the food chain will affect our health. The threshold value of the Cd concentration in barley grain is 0.1 mg kg^{-1} , which is the most critical among major cereal crops (0.4 mg kg^{-1} for rice and 0.2 mg kg^{-1} for wheat (*Triticum* spp.; CODEX STAN 193-1995, 2013). However, little is known about the molecular mechanisms underlying the Cd uptake in barley. There is wide genotypic variation in Cd accumulation in barley grain, and a recent study with genome-wide association mapping detected several quantitative trait loci

controlling Cd accumulation in different organs (Wu et al., 2015). However, the genes responsible for Cd accumulation have not been identified in barley. In this study, we found that Cd uptake is also mediated by *HvNramp5* because knockdown of *HvNramp5* decreased Cd accumulation in barley (Fig. 5, E and F). This

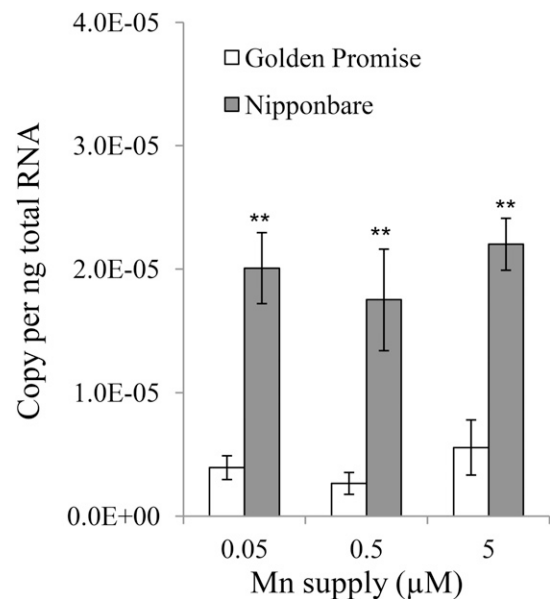


Figure 8. Comparison of *HvNramp5* and *OsNramp5* expression level in the root between barley and rice. The expression level of *HvNramp5* and *OsNramp5* in the roots was compared between barley (cv Golden Promise) and rice (cv Nipponbare) by absolute quantitative real-time PCR using common primers. Rice and barley were grown in nutrient solutions containing 0.05, 0.5, or 5 μM Mn for 7 d and then the roots were sampled for RNA extraction and gene expression analysis. Data are means \pm SD of three biological replicates and ** indicates significant difference at $P < 0.01$ by Student's t test.

means that Mn and Cd share the same transporter for the uptake. This is supported by competitive interaction between Mn and Cd for the uptake; increasing Mn in the external solution decreased Cd accumulation and vice versa (Figs. 5 and 6). In rice, Mn and Cd also share the same transporter, OsNramp5, for the uptake (Ishimaru et al., 2012; Ishikawa et al., 2012; Sasaki et al., 2012), although HvNramp5 differs from OsNramp5 in terms of expression patterns, tissue localization, and specificity of transport substrate as discussed below.

Different from Cd and Mn, which are taken up in an ionic form, Fe is taken up in the form of Fe(III)-phytosiderophore complex, which is transported by HvYS1 localized at the epidermal cells of barley roots (Murata et al., 2006). This may explain why HvNramp5 is not involved in Fe uptake (Fig. 5, C and D).

Different Uptake System for Mn and Cd between Rice and Barley

Rice is usually cultivated under anaerobic conditions, where Mn concentration in soil solution is very high due to soil reduction (Sasaki et al., 2011), while barley is an upland plant, which is cultivated in low Mn conditions (Pedas et al., 2005). Although both OsNramp5 in rice and HvNramp5 in barley mediate Mn uptake by the roots (Sasaki et al., 2012, Fig. 5), rice takes up and accumulates much more Mn than barley (Fig. 7). This difference could be attributed to their different expression pattern, tissue, and cellular localization. *OsNramp5* showed higher expression than *HvNramp5* at all Mn supply conditions tested (Fig. 8). Furthermore, in contrast to *OsNramp5*, which is highly expressed in the basal region of the rice roots (Sasaki et al., 2012), *HvNramp5* is highly expressed in the barley root tips (Fig. 1B). In the barley root tips, HvNramp5 is localized to the epidermal cells without polarity (Fig. 3A), while OsNramp5 in rice is polarly localized at the distal side of the exodermises and endodermis of the basal root region (Sasaki et al., 2012). Recently, a Mn efflux transporter (OsMTP9) has been identified in rice, which is localized at the proximal side of both the exodermis and endodermis (Ueno et al., 2015). Rice basal roots are characterized by two Casparian strips: one at the exodermis and one at the endodermis, and by formation of aerenchyma (Ma et al., 2006; Yamaji and Ma, 2007). A recent study showed that both Casparian strips and polar localization of influx and efflux transporters are required for efficient Si uptake in rice (Sakurai et al., 2015). Rice has a similar uptake system for Mn to that for Si, constructing an efficient uptake system by cooperative transporters OsNramp5-OsMTP9 (Ueno et al., 2015). By contrast, in barley root tips, the Casparian strip is usually weakly developed at the endodermis and there is no formation of aerenchyma. Therefore, Mn taken up through HvNramp5 at the epidermal cells is radially transported to the stele symplastically with less efficiency compared with rice uptake system. In barley roots, an efflux Si transporter

(HvLsi2) localized at the endodermis was found to be required for further releasing Si to the xylem (Mitani et al., 2009), but it is unknown whether there is a similar efflux transporter for Mn like OsMTP9 in barley. According to the barley genome database (<http://webblast.ipk-gatersleben.de/barley/>), a close homolog with 85% identity of OsMTP9 was found in barley. Its function and role in Mn uptake needs to be examined and compared with OsMTP9 in future.

Although HvNramp5 shares 84% identity with OsNramp5, there is some difference in the specificity of transport substrates between OsNramp5 and HvNramp5; OsNramp5 transports Mn^{2+} , Fe^{2+} , and Cd^{2+} in yeast (Ishimaru et al., 2012; Ishikawa et al., 2012), while HvNramp5 transports Mn^{2+} and Cd^{2+} , but not Fe^{2+} (Fig. 2). Knockout of *OsNramp5* resulted in decreased accumulation of Mn, Fe, and Cd when the plants were grown in nutrient solution (Sasaki et al., 2012). By contrast, knockdown of *HvNramp5* resulted in decreased Mn and Cd concentration in the roots and shoots, but the Fe concentration was unaffected (Fig. 5, C and D). In addition to HvNramp5 and OsNramp5, other Nramp members also show different specificity. For example, OsNramp3 only transports Mn, but not Cd and Fe (Yamaji et al., 2013), while OsNramp4 (OsNramp4) transports trivalent Al ion (Xia et al., 2010). The mechanism underlying this specificity of transport substrate remains to be examined in future. Recently, three residues of AtNramp4 have been identified to be involved in metal selectivity in Arabidopsis (Pottier et al., 2015).

In conclusion, HvNramp5 is a plasma membrane-localized transporter for Mn and Cd. It is constitutively expressed in the root epidermal cells and responsible for Mn and Cd uptake in barley.

MATERIALS AND METHODS

Cloning of Full-Length cDNA of *HvNramp5*

To isolate the full-length cDNA sequence of *HvNramp5*, total RNA was extracted from barley (*Hordeum vulgare* cv Golden Promise) roots using the RNeasy Plant Mini Kit (Qiagen). The total RNA was then converted to cDNA according to the protocol supplied by the manufacturers of SuperScript II (Invitrogen). The full-length cDNA was amplified by the PCR using primers 5'-TACGTTCACGCAAAGGGACA-3' and 5'-ACGTATACACGGTCCGACAG-3', which were designed based on a reference sequence of AK364374 by blasting the mRNA sequence of *OsNramp5* (Sasaki et al., 2012), found in the barley genome database (<http://webblast.ipk-gatersleben.de/barley/>). The fragment amplified was then introduced into the pGEM vector by pGEM-T (Easy) Vector Systems (Promega) for sequencing. The sequence of the amplified fragments was confirmed by a sequence analyzer (ABI Prism 310 genetic analyzer; Applied Biosystems) using the Big Dye Terminators V3.1 cycle sequencing kit.

Phylogenetic Analysis

Amino acid sequence of HvNramp5 from barley cultivar Golden Promise was translated by software DNASTAR (<http://www.dnastar.com/>), based on the full-length cDNA sequence. Transmembrane domains of HvNramp5 were predicted by SOSUI, ver. 1.11, software (<http://bp.nuap.nagoya-u.ac.jp/sosui/>). For phylogenetic analysis, peptide sequence alignment was analyzed by ClustalW software (<http://clustalw.ddbj.nig.ac.jp/>), comparing HvNramp5 with seven Nramp proteins in rice (*Oryza sativa*), including OsNramp1 (LOC_Os07g15460), OsNramp2 (LOC_Os03g11010), OsNramp3 (LOC_Os06g46310),

OsNramp4 (LOC_Os02g03900), OsNramp5 (LOC_Os07g15370), OsNramp6 (LOC_Os01g31870), and OsNramp7 (LOC_Os12g39180). The phylogenetic tree was constructed with MEGA 5 software (<http://www.megasoftware.net/>) after ClustalW alignment.

Yeast Experiments

The cDNA fragment containing an entire ORF of *HvNramp5* was amplified by RT-PCR using the primers 5'-TTTAAGCTTAAAATGGAGATCGA-GAGGAGGC-3' and 5'-TTTCTCGAGCTACTGCATATCTCTAGTGC-3', containing the *Hind*III and *Xho*I restriction sites, respectively. The cDNA fragment of *HvIRT1* ORF was also amplified by RT-PCR using the primers 5'-TTTAAGCTTAAAATGTCGTCGTCGTCGTCG-3' and 5'-TTTGGCGCCGCT-CACGCCATTGGCCATG-3', containing *Hind*III and *Not*I restriction site, respectively. These fragments were cloned into a pYES2 vector (Invitrogen). After sequence confirmation, both the constructed plasmids and the empty vector were introduced into different yeast strains according to the manufacturer's protocols (S.C. Easy Comp Transformation Kit; Invitrogen). The yeast strains used in this study were BY4741, the Mn uptake-deficient mutant $\Delta smf1$, and the Fe uptake-deficient double-mutant DDY4 ($\Delta fet3fet4$), as described by Yamaji et al. (2013).

Complementation of the $\Delta smf1$ and DDY4 phenotypes and evaluation of Cd tolerance in yeast (BY4741, a wild-type strain) were performed according to Yamaji et al. (2013) with some modifications. We supplemented with 0 or 1.5 mM EGTA in the growth medium for $\Delta smf1$, 0 or 12 mM BPDS in the growth medium for DDY4, and 0 or 30 μ M CdCl₂ in the growth medium for BY4741. After spotting at different yeast-cell dilutions (optical densities at 600 nm of 0.2, 0.02, 0.002, and 0.0002), plates were incubated for 3 to 5 d at 30°C and then the plates were photographed.

For liquid experiment of Cd uptake in yeast (BY4741), each transformant was precultured overnight in liquid medium containing 2% Glc, 0.67% yeast nitrogen base without amino acids, and 0.2% appropriate amino acids. Yeast cells were pelleted by centrifugation and washed three times with Milli-Q water (Millipore), and the resulting pellets were resuspended in the same liquid medium (control) in the presence of 5 μ M CdCl₂ or in another liquid medium containing 2% Gal, 0.67% yeast nitrogen base without amino acids, 0.2% appropriate amino acids, and 5 μ M CdCl₂. The uptake experiment was done at 30°C with shaking horizontally at 200 rpm for 4 h and cells were washed three times by Milli-Q water (Millipore) at the end of the experiment. The dry weight of yeast cells was recorded after drying 24 h at 70°C in an oven and the yeast was extracted with a 5% HNO₃ for Cd measurement. All yeast experiments were conducted at least two times independently and yielded the similar results.

Expression Pattern of *HvNramp5*

For spatial expression of *HvNramp5*, the roots of barley (cv Golden Promise) grown in a 0.5 mM CaCl₂ solution for 4 d, were separated into different segments (0–5, 5–10, 10–20 mm) with a razor. To investigate tissue specific expression of *HvNramp5*, cDNA samples of central cylinder and outer tissues, which were prepared before (Fujii et al., 2012), were used. The samples were collected from the root tip section (2 mm) of barley (cv Morex) using a Veritas Laser Microdissection System LCC1704 (Molecular Devices). To determine the effect of metal deficiency on *HvNramp5* expression, seedlings (2-week-old) were transferred to one-fifth Hoagland's solution with or without each essential metal including Fe, Zn, Cu, and Mn. To determine the effect of Cd addition on *HvNramp5* expression, a final concentration of 0.5 μ M CdSO₄ was added to the nutrient solution as described below. Culture solution was renewed every 2 d. After 7 d of metal depletion or Cd treatment, root and shoot samples were harvested separately for RNA extraction and gene expression analysis. Extraction of total RNA was as same as described above. Specific cDNAs were amplified by SYBR premix EX Taq (TAKARA) and quantitative real-time RT-PCR (ABI Prism 7500; Applied Biosystems) with the following primer sets: 5'-TCCCTCGCTACCTGGAT-3' and 5'-GCTTCGGATACTCGTCTT-3' for *HvNramp5*; and 5'-GACTCTGGTCATGGTGTGTCAGC-3' and 5'-GGCTGGAA-GAGGACCTCAGG-3' for *Actin* as an internal standard. The relative expression was normalized based on these two genes by the 2^{ΔΔCt} method using the CFX Manager software (Bio-Rad).

Subcellular and Cellular Localization of *HvNramp5*

For observation of the subcellular localization of *HvNramp5*, *HvNramp5* cDNA containing *Sal*I and *Nco*I restriction sites, but not the stop codon, was amplified by RT-PCR using the primers

5'-TTGTCGACATGGAGATCGAGAGGGAGGC-3' and 5'-TTTCCATGGGCTG-CATATCTCTAGTGTCT-3'. After sequence confirmation, the amplified cDNA fragment was then subcloned in-frame in front of the GFP-coding region in a pBluescript vector, producing the *HvNramp5*-GFP construct under the control of the 35S promoter. RFP was used as a marker of cytosol and nucleus (Matz et al., 1999). Gold particles with a diameter of 1 μ m coated with *HvNramp5*-GFP or GFP alone and RFP were introduced into onion (*Allium cepa* L.) epidermal cells via particle bombardment (PDS1000/He particle delivery system; Bio-Rad) using 1100 psi rupture disks. After incubation in the dark at room temperature for 16 h, the fluorescence was observed by confocal laser scanning microscopy (LSM700; Carl Zeiss).

To examine the cellular localization, the synthetic peptide MEIEREAPGSEGRGRSWRAN-C (positions 1–19 of *HvNramp5* amino acids) was used to immunize rabbits to obtain antibodies against *HvNramp5*. The obtained antiserum was purified through a peptide affinity column before use. Different root cross sections (2 mm and 15 mm from the root tip) from 10-d-old seedlings of cultivar Golden Promise were used for immunostaining of *HvNramp5* according to Sasaki et al. (2012). Fluorescence of the secondary antibody (Alexa Fluor 555 goat anti-rabbit IgG; Molecular Probes) was observed with a confocal laser scanning microscope (LSM700; Carl Zeiss).

Barley Transformation and Knockdown Mutant Identification

To generate the hairpin RNAi construct, we cloned a 244 bp fragment (–5 to 239 bp from ATG) of *HvNramp5* cDNA as inverted repeats into the pANDA vector (Miki and Shimamoto, 2004) under control of the maize (*Zea mays*) ubiquitin 1 promoter and subsequently transformed the vector into *Agrobacterium tumefaciens* (strain EHA101). The primer sequences used for amplifying a 244-bp fragment of *HvNramp5* cDNA were 5'-AAAAAGCAGGCTCGGCAATGGAGATCGAGAGG-3' and 5'-AGAAAGCTGGGTTATCTGTGATTGCTCCGGC-3'. Immature embryos of barley cultivar Golden Promise were used for *Agrobacterium*-mediated transformation. Transformation was basically performed using the protocols of Hensel et al. (2008), Hiei et al. (2006), and Hiei and Komari (2006).

After PCR confirmation using the primers 5'-GTCTCGGTGAA-CAGGTATGG-3' and 5'-AGAAAGCTGGGTTATCTGTGATTGCTCCGGC-3', we obtained several independent transgenic lines, and two independent transgenic homozygous lines (T2 generation) of them were used for further analysis. The expression levels of *HvNramp5* and *HvIRT1* were determined in the roots of the RNAi lines, the homozygous wild type from transgenic plants (RNAi-wild type), and Golden Promise (wild type), using real-time RT-PCR. The primers used for *HvIRT1* were 5'-CCAGATGTTTGAGGGATGG-3' and 5'-GATAGACACAAGACACACC-3', and the primers for *HvNramp5* and *Actin* were the same as described above.

Plant Materials and Growth Condition

Seeds of wild-type barley (cv Golden Promise) and RNAi lines were soaked in deionized water for 2 h, and then incubated overnight on a moist paper in the dark at 23°C. Germinated seeds were transferred to a nylon mesh floating on a continuously aerated solution in a 1.5-L plastic container containing 0.5 mM CaCl₂ (pH 5.6) in the dark. After a 4-d culture, the seedlings were then transferred into an aerated one-fifth Hoagland's solution (pH 6.0). The solution contained 1 mM KNO₃, 1 mM Ca(NO₃)₂, 0.4 mM MgSO₄, and 0.2 mM NH₄H₂PO₄, and micronutrients comprising 20 μ M Fe-EDTA, 3 μ M H₂BO₃, 1.0 μ M (NH₄)₆Mo₇O₂₄, 0.5 μ M MnCl₂, 0.4 μ M ZnSO₄, and 0.2 μ M CuSO₄. All plants were grown in a growth chamber at 23°C of 14 h d/18°C of 10 h night. Culture solution was renewed every 2 d.

For phenotypic analysis of the *HvNramp5* RNAi lines, the seedlings of two transgenic homozygous RNAi lines, the homozygous wild type, and the Golden Promise were grown in a one-fifth Hoagland's solution with different concentrations of Mn (0.05, 0.5, and 5 μ M) as MnCl₂ or Cd (0.1, 0.5, and 1 μ M) as CdSO₄, or Fe (0.1, 2, and 10 μ M) as FeSO₄. The Cd concentration in the solution for different Mn and Fe treatments was 0.1 μ M. After 14 d, the roots were washed three times with 5 mM CaCl₂ and separated from the shoots. The samples were dried at 70°C for 2 d and used for metal concentration determination as described below.

For comparing Mn accumulation and *Nramp5* expression level between barley and rice, seedlings of barley (cv Golden Promise) and rice (cv Nipponbare) were grown in one-fifth Hoagland's solution as mentioned above for barley and one-half-strength Kimura B solution for rice

containing 0.05, 0.5 or 5 μM Mn, respectively. After exposure for 7 d, the roots and shoots were sampled for Mn concentration determination. The fresh roots were also used for RNA extraction and absolute expression analysis as described below.

Absolute Expression Analysis of *Nramp5* in Barley and Rice

After alignment of the cDNA sequences of *Nramp5* genes in barley and rice, a 362 bp identical fragment was amplified from cv Golden Promise using common primers (5'-CTCTGGGTGATTCTGATTG-3' and 5'-CTCAGTCCCCGAAGAAG-3'). The fragment amplified was then introduced into the pGEM vector by pGEM-T (Easy) Vector Systems (Promega). To generate standard curves for absolute quantification, a series of dilutions (from 1×10^{-1} to 10^{-6} ng) of the plasmids prepared were made and then assayed by real-time PCR. C_T values for each sample were converted into absolute copy numbers using the standard curves. The expression levels of *Nramp5* in the roots of barley and rice were quantified by absolute quantitative real-time PCR using the common primers.

Metal Concentration Determination

After being dried in an oven at 70°C for 2 d, samples were digested in concentrated nitric acid at 140°C. The concentration of mineral elements including Mn, Fe, Cu, Zn, and Cd in the digest solution was determined by ICP-MS (7700X; Agilent Technologies) after dilution as described by Wu et al. (2015).

Statistical Analysis

Significance analysis was performed by Student's *t* test or Tukey's test using SPSS software (IBM SPSS Statistics Ver. 16). The difference at $P < 0.05$ and $P < 0.01$ was considered as significant and highly significant, respectively.

Accession Numbers

Sequence data from this article can be found in the GenBank/EMBL data libraries under accession number LC184278.

Supplemental Data

The following supplemental materials are available.

Supplemental Figure S1. Sequence, gene, and protein structure, and phylogenetic analysis of *HvNramp5*.

Supplemental Figure S2. Gene expression level in the roots of *HvNramp5* RNAi lines and wild types.

Supplemental Figure S3. Concentration of Cu and Zn in the *HvNramp5* RNAi lines at different Mn concentrations.

Supplemental Figure S4. Phenotypic analysis of *HvNramp5* RNAi lines at different Cd concentrations.

Supplemental Figure S5. Phenotypic analysis of *HvNramp5* RNAi lines at different Fe concentrations.

Received August 1, 2016; accepted September 8, 2016; published September 12, 2016.

LITERATURE CITED

Bereczky Z, Wang HY, Schubert V, Ganai M, Bauer P (2003) Differential regulation of *nramp* and *irt* metal transporter genes in wild type and iron uptake mutants of tomato. *J Biol Chem* **278**: 24697–24704

Cailliatte R, Lapeyre B, Briat JF, Mari S, Curie C (2009) The NRAMP6 metal transporter contributes to cadmium toxicity. *Biochem J* **422**: 217–228

Cailliatte R, Schikora A, Briat JF, Mari S, Curie C (2010) High-affinity manganese uptake by the metal transporter NRAMP1 is essential for *Arabidopsis* growth in low manganese conditions. *Plant Cell* **22**: 904–917

CODEX STAN 193-1995 (2013) General standard for contaminants and toxins in foods and feed. www.fao.org/input/download/standards/17/CXS_193e_2015.pdf (accessed March 10, 2015)

Curie C, Alonso JM, Le Jean M, Ecker JR, Briat JF (2000) Involvement of NRAMP1 from *Arabidopsis thaliana* in iron transport. *Biochem J* **347**: 749–755

Engl A, Kunz B (1995) Biosorption of heavy metals by *Saccharomyces cerevisiae*: effects of nutrient conditions. *J Chem Technol Biotechnol* **63**: 257–261

Fujii M, Yokosho K, Yamaji N, Saisho D, Yamane M, Takahashi H, Sato K, Nakazono M, Ma JF (2012) Acquisition of aluminium tolerance by modification of a single gene in barley. *Nat Commun* **3**: 713–721

Hall JL, Williams LE (2003) Transition metal transporters in plants. *J Exp Bot* **54**: 2601–2613

Hensel G, Valkov V, Middlefell-Williams J, Kumlehn J (2008) Efficient generation of transgenic barley: the way forward to modulate plant-microbe interactions. *J Plant Physiol* **165**: 71–82

Hiei Y, Ishida Y, Kasaoka K, Komari T (2006) Improved frequency of transformation in rice and maize by treatment of immature embryos with centrifugation and heat prior to infection with *Agrobacterium tumefaciens*. *Plant Cell Tiss Org* **87**: 233–243

Hiei Y, Komari T (2006) Improved protocols for transformation of indica rice mediated by *Agrobacterium tumefaciens*. *Plant Cell Tiss Org* **85**: 271–283

Mayer KF, Waugh R, Brown JW, Schulman A, Langridge P, Platzer M, Fincher GB, Muehlbauer GJ, Sato K, Close TJ, Wise RP, Stein N (2012) A physical, genetic and functional sequence assembly of the barley genome. *Nature* **491**: 711–716

Ishikawa S, Ishimaru Y, Igura M, Kuramata M, Abe T, Senoura T, Hase Y, Arai T, Nishizawa NK, Nakanishi H (2012) Ion-beam irradiation, gene identification, and marker-assisted breeding in the development of low-cadmium rice. *Proc Natl Acad Sci USA* **109**: 19166–19171

Ishimaru Y, Takahashi R, Bashir K, Shimo H, Senoura T, Sugimoto K, Ono K, Yano M, Ishikawa S, Arai T, Nakanishi H, Nishizawa NK (2012) Characterizing the role of rice NRAMP5 in manganese, iron and cadmium transport. *Sci Rep* **2**: 286

Kaiser BN, Moreau S, Castelli J, Thomson R, Lambert A, Bogliolo S, Puppo A, Day DA (2003) The soybean NRAMP homologue, GmDMT1, is a symbiotic divalent metal transporter capable of ferrous iron transport. *Plant J* **35**: 295–304

Lanquar V, Lelièvre F, Bolte S, Hamès C, Alcon C, Neumann D, Vansuyt G, Curie C, Schröder A, Krämer U, Barbier-Brygoo H, Thomine S (2005) Mobilization of vacuolar iron by AtNRAMP3 and AtNRAMP4 is essential for seed germination on low iron. *EMBO J* **24**: 4041–4051

Lanquar V, Ramos MS, Lelièvre F, Barbier-Brygoo H, Krieger-Liszskay A, Krämer U, Thomine S (2010) Export of vacuolar manganese by AtNRAMP3 and AtNRAMP4 is required for optimal photosynthesis and growth under manganese deficiency. *Plant Physiol* **152**: 1986–1999

Ma JF, Tamai K, Yamaji N, Mitani N, Konishi S, Katsuhara M, Ishiguro M, Murata Y, Yano M (2006) A silicon transporter in rice. *Nature* **440**: 688–691

Matz MV, Fradkov AF, Labas YA, Savitsky AP, Zaraisky AG, Markelov ML, Lukyanov SA (1999) Fluorescent proteins from nonbioluminescent Anthozoa species. *Nat Biotechnol* **17**: 969–973

Miki D, Shimamoto K (2004) Simple RNAi vectors for stable and transient suppression of gene function in rice. *Plant Cell Physiol* **45**: 490–495

Milner MJ, Mitani-Ueno N, Yamaji N, Yokosho K, Craft E, Fei Z, Ebbs S, Clemencia Zambrano M, Ma JF, Kochian LV (2014) Root and shoot transcriptome analysis of two ecotypes of *Nocca caerulescens* uncovers the role of Nramp1 in Cd hyperaccumulation. *Plant J* **78**: 398–410

Mitani N, Chiba Y, Yamaji N, Ma JF (2009) Identification and characterization of maize and barley Lsi2-like silicon efflux transporters reveals a distinct silicon uptake system from that in rice. *Plant Cell* **21**: 2133–2142

Mizuno T, Usui K, Horie K, Nosaka S, Mizuno N, Obata H (2005) Cloning of three ZIP/Nramp transporter genes from a Ni hyperaccumulator plant *Thlaspi japonicum* and their Ni²⁺-transport abilities. *Plant Physiol Biochem* **43**: 793–801

Murata Y, Ma JF, Yamaji N, Ueno D, Nomoto K, Iwashita T (2006) A specific transporter for iron(III)-phytosiderophore in barley roots. *Plant J* **46**: 563–572

Nevo Y, Nelson N (2006) The NRAMP family of metal-ion transporters. *Biochim Biophys Acta* **1763**: 609–620

Olsen LI, Palmgren MG (2014) Many rivers to cross: the journey of zinc from soil to seed. *Front Plant Sci* **5**: 30

- Oomen RJ, Wu J, Lelièvre F, Blanchet S, Richaud P, Barbier-Brygoo H, Aarts MG, Thomine S (2009) Functional characterization of NRAMP3 and NRAMP4 from the metal hyperaccumulator *Thlaspi caerulescens*. *New Phytol* **181**: 637–650
- Pedas P, Heberlein CA, Schjoerring JK, Holm PE, Husted S (2005) Differential capacity for high-affinity manganese uptake contributes to differences between barley genotypes in tolerance to low manganese availability. *Plant Physiol* **139**: 1411–1420
- Pedas P, Ytting CK, Fuglsang AT, Jahn TP, Schjoerring JK, Husted S (2008) Manganese efficiency in barley: identification and characterization of the metal ion transporter HvIRT1. *Plant Physiol* **148**: 455–466
- Pottier M, Oomen R, Picco C, Giraudat J, Scholz-Starke J, Richaud P, Carpaneto A, Thomine S (2015) Identification of mutations allowing Natural Resistance Associated Macrophage Proteins (NRAMP) to discriminate against cadmium. *Plant J* **83**: 625–637
- Sakurai G, Satake A, Yamaji N, Mitani-Ueno N, Yokozawa M, Feugier FG, Ma JF (2015) In silico simulation modeling reveals the importance of the Casparian strip for efficient silicon uptake in rice roots. *Plant Cell Physiol* **56**: 631–639
- Sasaki A, Yamaji N, Ma JF (2016) Transporters involved in mineral nutrient uptake in rice. *J Exp Bot* **67**: 3645–3653
- Sasaki A, Yamaji N, Xia J, Ma JF (2011) OsYSL6 is involved in the detoxification of excess manganese in rice. *Plant Physiol* **157**: 1832–1840
- Sasaki A, Yamaji N, Yokosho K, Ma JF (2012) Nramp5 is a major transporter responsible for manganese and cadmium uptake in rice. *Plant Cell* **24**: 2155–2167
- Takahashi R, Ishimaru Y, Senoura T, Shimo H, Ishikawa S, Arai T, Nakanishi H, Nishizawa NK (2011) The OsNRAMP1 iron transporter is involved in Cd accumulation in rice. *J Exp Bot* **62**: 4843–4850
- Thomine S, Wang R, Ward JM, Crawford NM, Schroeder JI (2000) Cadmium and iron transport by members of a plant metal transporter family in *Arabidopsis* with homology to Nramp genes. *Proc Natl Acad Sci USA* **97**: 4991–4996
- Ueno D, Sasaki A, Yamaji N, Miyaji T, Fujii Y, Takemoto Y, Moriyama S, Che J, Moriyama Y, Iwasaki K, Ma JF (2015) A polarly localized transporter for efficient manganese uptake in rice. *Nat Plants* **1**: 15170
- Wu D, Sato K, Ma JF (2015) Genome-wide association mapping of cadmium accumulation in different organs of barley. *New Phytol* **208**: 817–829
- Xia J, Yamaji N, Kasai T, Ma JF (2010) Plasma membrane-localized transporter for aluminum in rice. *Proc Natl Acad Sci USA* **107**: 18381–18385
- Xiao H, Yin L, Xu X, Li T, Han Z (2008) The iron-regulated transporter, MbNRAMP1, isolated from *Malus baccata* is involved in Fe, Mn and Cd trafficking. *Ann Bot (Lond)* **102**: 881–889
- Yamaji N, Ma JF (2007) Spatial distribution and temporal variation of the rice silicon transporter Lsi1. *Plant Physiol* **143**: 1306–1313
- Yamaji N, Sasaki A, Xia JX, Yokosho K, Ma JF (2013) A node-based switch for preferential distribution of manganese in rice. *Nat Commun* **4**: 2442
- Yokosho K, Yamaji N, Ueno D, Mitani N, Ma JF (2009) OsFRDL1 is a citrate transporter required for efficient translocation of iron in rice. *Plant Physiol* **149**: 297–305